https://doi.org/10.48047/AFJBS.6.15.2024.11691-11715

African Journal of Biological Sciences

Journal homepage: http://www.afjbs.com

Research Paper Open Access

Induction of cytotoxicity and cell cycle arrest in human prostate cancer cells by chitosan nanoparticles encapsulating *Andrographis serpyllifolia* (Rottler ex Vahl) Wight extract.

Hemalatha Ravikumar[1], Kavimani Thangasamy[1], Sradha Sajeev[1], Anju Rani George[1], Menaga Suriyakanthan[1], Madhu Priya Govindhan Anbazhagan[1], Natesan Geetha[1*]

DEPARTMENT AND INSTITUTION**:** Research Scholar, Department of Botany, Bharathiar University, Coimbatore- 641046, Tamil Nadu, India.
Email id: kavieswari007@gmail.com, sajeevsradha@gmail.com, anjuranigeorge94@gmail.com, menaga2620@gmail.com, madhumaha2919@gmail.com.
CORRESPONDING AUTHOR: Natesan Geetha[1*]
Address: Professor, Department of Botany, Bharathiar University, Coimbatore- 641046, Tamil Nadu, India.
***Email id:** ngeethaptc@gmail.com
Phone no: 7010663900

Volume 6, Issue 15, Sep 2024

Received: 15 July 2024

Accepted: 25 Aug 2024

Published: 25 Sep 2024

doi: 10.48047/AFJBS.6.15.2024.11691-11715

ABSTRACT
Prostate cancer is the second most common cause of death for men worldwide. The encapsulation of herbal extract in polymeric nanoparticles is a prominent therapeutic remedy and targeted drug delivery for cancer. The aim of the present study was to investigate the cytotoxicity and cell cycle arrest of human prostate cancer cells by using chitosan nanoparticles encapsulated *Andrographis serpyllifolia* extract. Aqueous extract of *A. serpyllifolia* (ALE) at various concentrations were encapsulated with 2% (w/v) chitosan nanoparticles (ALE CSNPs). Initially, entrapment efficiency of ALE by CSNPs and drug release percentage from CSNPs were determined and then ALE CSNPs were subjected to various spectroscopic characterization. The effect of ALE CSNPs on PC3 cells was examined by MTT assay and flow cytometry DNA analysis. Among, various concentrations *of* ALE CSNPs, 0.25 mg/mL concentration exhibited higher entrapment percentage (87.73%). *In vitro* drug release study showed a controlled and sustained crude drug release from ALE CSNPs (91.30%) within 5.5 hours. The addition of plant extract onto chitosan nanoparticles increases the size of the nanoparticles of ALE CSNPs i.e. 22.3 nm compared to control i.e. 29.3 nm which is confirmed by XRD. SEM image revealed the synthesized ALE CSNPs had huge surface area. Compared to CSNPs, ALE CSNPs showed decreased cell viability and increased percentage of obstructed cells at G0/G1 cell cycle phase effectively. In conclusion, ALE CSNPs act as a promising drug delivery system using chitosan nanocarrier for targeted release of *A. serpyllifolia* leaf aqueous extract to PC3 cell lines.

Keywords*:* Prostate cancer, chitosan nanoparticles, *Andrographis serpyllifolia*, cytotoxicity, cell cycle arrest.

INTRODUCTION

Prostate cancer is the second most commonly second eventuating cancer in men and the fourth most common cancer altogether. Nanoscale drug-delivery systems for cancer therapeutics are rapidly evolving and may provide a novel strategy [1]. In cancer chemotherapy, nanoparticle-based drug carriers have garnered a lot of interest due to their numerous advantages, which include improved chemo drug solubility in water, longer blood circulation times, higher cellular uptake, and improved accumulation in tumors. In recent years, nanotechnology that combines with polymers has a tremendous interest in pharmaceuticals industry along with therapeutic innovations. Polymeric nanoparticles offer a new advancement in drug discovery and can be prepared either from synthetic or natural polymers. Chitosan nanoparticles (ChNPs) are the drug carriers that have the capacity to release the encapsulated drug gradually due to their high stability, biodegradability and quick intracellular transit. Because of its chemical makeup, chitosan is a material that shows promise for use in polyphenol nano-delivery systems and as a safe agent for drug loading and release [2]. Biologically active compounds with a synergistic effect are produced when polyphenols, which have at least one aromatic ring and –OH groups with at least one ring–are combined with chitosan nanoparticles [3].

Andrographis serpyllifolia (Rottler ex Vahl) Wight, a member of the family Acanthaceae, is a valuable medicinal plant with significant therapeutic activity and is found incorporated in several ethnobotanical formulations. *A. serpyllifolia* is densely hispid prostrate herb endemic to peninsular India. *A. serpyllifolia* has evolved into a ground hugging prostrate, perennial, geophyte that successfully survives multiple geo-ecological challenges and grazing threats year after year. The bioactive compounds of *A. serpyllifolia* are related to have important biological applications such as antiulcer, anti-diabetic, [4] antipyretic, anti-inflammatory, antimicrobial, anticancer and antidote [5]. According to [6] phenolics and andrographolide present in aqueous extract of *A. serpyllifolia* may be the factor responsible for anticancer properties. Effective

antiproliferative and DNA protective activities are due to free and bound phenolics of *A. serpyllifolia* [7]. Based on previous literature, there is no study on cytotoxicity and cell cycle arrest of human prostate (PC3) cell line induced by *A. serpyllifolia* aqueous leaf extract loaded with chitosan nanoparticles. Therefore, the present investigation was undertaken.

MATERIALS AND METHODS

Chemicals

Medium molecular weight chitosan (190-310 kDa MW with 75-85% degree of deacetylation) and dialysis membrane bags were purchased from Sigma-Aldrich. Glacial acetic acid, Sodium tripolyphosphate and phosphate buffer (pH 7.4) were procured from Sisco Research Laboratories (Mumbai, India).

Collection, Identification and Extraction process of the plant

A. serpyllifolia was collected from Dharmapuri district, Tamil Nadu India. The identification and authentification of the plant was done in Botanical survey of India Coimbatore district, Tamil Nadu (BSI/SRC/5/23/2023/Tech). Leaf samples were collected from mature plant and cut into small pieces and washed under running water to remove adhering debris. Then the samples were dried under shade and ground into fine powder and stored at 4^{o}C. 10 grams of leaf powder were taken and mixed in 100 ml of distilled water. The mixture was boiled at 80°C for 30 minutes in water bath and cooled at room temperature. Then, the extract was filtered through Whatman No. 1 filter paper. The collected filtrate was dried and stored in refrigerator till further use.

Synthesis of ALE encapsulated chitosan nanoparticles (ALE CSNPs)

ALE CSNPs were prepared according to the ionic gelation method [8]. Briefly, chitosan (2% w/v) was dissolved in dilute acetic acid (1% v/v) overnight at room temperature to form a 2 mg/2 mL concentration solution and pH was adjusted to 5 using 1 M NaOH. Sodium tripolyphosphate (TPP) was dissolved in water to reach a final concentration of 1 mg/mL. ALE solution was

prepared by dissolving the filtrate at a concentration of 10 mg/10 mL. Different concentrations of ALE (0.25, 0.75, 0.5 and 1.0 mg) was mixed with 1 mL of TPP separately. Next, this mixture was added to 1 ml of chitosan solution to reach a final mass ratio of 3:1 (chitosan:TPP) and then left to stir for 45 min. The mixtures were centrifuged at 10000 rpm for 15 min and washed twice with de-ionized water. After centrifugation, the supernatants were discarded and the pellets containing ALE CSNPs were stored in the refrigerator at 4°C for further use.

Determination of Entrapment Efficiency (EE %)

The amount of ALE encapsulated within the CSNPs was determined by indirect method, through calculating the amount of unencapsulated drug. After adding the TPP, the mixture was centrifuged at 10000 rpm for 15 min and the clear supernatant containing the free unencapsulated drug was collected, diluted with distilled water and measured spectrophotometrically at 273 nm [9]. The drug (ALE) entrapment efficiency in CSNPs was determined using the following equation.

$$EE\% = \frac{\text{(Total amount of ALE added- free ALE in supernatant)}}{\text{Total ALE added}} \times 100$$

Determination of *in vitro* drug release percentage

ALE release percentage from CSNPs was determined using the technique of dialysis tube analysis (12,000-14,000 molecular weight). In brief, the dialysis membrane was washed with lukewarm double distilled water (70ºC) for 1hr and rinsed thoroughly (thrice) to eliminate glycerin. ALE CSNPs with higher entrapment efficiency (87.73%.) was placed in a dialysis bag

which was sealed and immersed in 50 mL of phosphate buffer (pH 7.4) at room temperature with stirring at 1000 rpm for 6 h. 3 mL of the solution was withdrawn every half an hour and replaced with an equivalent volume of fresh solution. This process was repeated upto 3.5 hours. The withdrawn samples were analyzed using UV/visible spectroscopy at 265 nm and the amount of ALE release pattern from CSNPs was determined [10]. The drug release percentage was determined by using the following formula.

$$\text{Drug release [\%]} = C(t)/C(0) \times 100$$

where C(t) is the absorbance of ALE CSNPs at 265 nm at time t.

In vitro drug release kinetics

Various release kinetic models such as zero order, first order, Higuchi model and Korsmeyer–Peppas have been used to fit the cumulative *in vitro* drug release data and to describe the drug release kinetics [11]. The best release pattern is explained using the coefficient of determination (R^2) value. Model with the highest R^2 is considered as the best one [12].

Characterization of drug loaded chitosan nanoparticles

CSNPs and ALE CSNPs were subjected to UV-vis spectrophotometry and Fourier transform infrared spectroscopy (FTIR) to study optical properties and to identify functional groups, respectively. Crystallinity patterns of CSNPs and ALE CSNPs were determined by X-ray diffraction (Shimadzu LabX- XRD 1600). Particle size, the charge on the surface of the nanoparticles and poly dispersity index (PDI) were measured through Dynamic Light Scattering (DLS) with zetasizer (Malvern analytical, Chennai India). Topography and elemental composition of CSNPs and ALE CSNPs were investigated through Scanning electron microscopy and Energy Dispersive analysis of X-Ray (Quanta 400 ESEM).

***In vitro* anti-prostate activity**

Human prostate cell lines (PC3) were obtained from American Type Culture Collection (ATCC) 10801. Cells were cultured in Dulbecco's Modified Eagle Medium (DMEM) media supplemented with 10% (*v/v*) fetal bovin serum and 1% (*v/v*), 100 U/Ml penicillin and 100 µg/mL streptomycin. Cells were cultured in an incubator at 37°C and 5% CO_2 humidified atmosphere. Medium was changed every 2 -3 days. Reagents and media for cell culture were purchased from Sigma-aldrich (Merck) and Sisco Research Laboratories Pvt. Ltd., Mumbai, India. The cellular toxicity on cultured cells was measured using MTT [3-(4,5-dimethylthiazol-2-yl)-2, 5-diphenyl tetrazolium bromide] assay. Cells were grown overnight in a 96-well plate at a density of 1×10^4 cells per well. Then, cells were treated with different concentrations of test samples such as ALE and ALE CSNPs (0, 10, 20, 40, 80, 160 and 320 µg/mL) and anticancer standard Doxorubicin (3.125, 6.25, 12.5, 25, 50, 100µM) and incubated at 37°C for 24 h. Later, cells were washed twice with phosphate buffer saline (PBS). MTT solution was added to each well (0.5 mg/mL) and the plate was incubated for 4h at 37° C in 5% CO_2 atmosphere. Finally, the medium was replaced by DMSO to solubilize the formazan. The absorbance was measured using a microplate reader at 590 nm. IC_{50} value for cytotoxicity tests were derived from a nonlinear regression analysis based sigmoid dose response curve and calculated using prism Graph Pad Prism 6 (Graph pad, SanDiego, CA, USA) [13].

The percentage growth inhibition was calculated using the following formula:

% inhibition = (control abs - sample abs) / (control abs) × 100

Cell morphological analysis

PC3 cancer cells were grown and incubated with CSNPs, Doxorubicin, ALE and ALE CSNPs at their IC50 concentration and cells were taken and observed under an inverted phase contrast microscope to study the cell morphology at 40× magnification (Vivek *et al*., 2012).

Flow Cytometric Analysis of Cell Cycle Distribution

Cell cycle distribution and ploidy status of cells after treatment with ALE and ALE CSNPs were determined by flow cytometry DNA analysis. At the end of treatments, cells were detached from the plates by the addition of 0.25% trypsin, washed in PBS, fixed in 70% ethanol at 4^{o}C and treated with 10 mg/ml RNAse for 30 minutes at 37^{o}C. The DNA content was evaluated in a FACS can flow cytometer (Becton Dickinson, Franklin Lakes, NJ) after staining the cells with 50 mg/ml propidium iodide for 15 minutes in the dark at room temperature and analyzed using Cell Quest software. For cell cycle analysis, only single cells were considered [14].

Statistical analysis

All statistical analysis was performed using Prism 5 (GraphPad Software, Inc.). Data are presented as the mean ± SEM. One-way ANOVA with Dunnett's post hoc test was used to compare across multiple treatments. Experiments were repeated three times with at least triplicate wells per condition. Results with $P < 0.05$ was considered to indicate a statistically significant difference. The SPSS software (ver. 22.0, SPSS Inc., United States) was used to analyze the experimental data.

RESULTS

Entrapment efficiency

The percentage of entrapment efficiency is illustrated in Fig 1. Among various concentrations of ALE CSNPs (0.25, 0.5, 0.75 and 1.0 mg/mL), 0.25 mg showed higher percentage of entrapment efficiency (87.73%) within CSNPs.

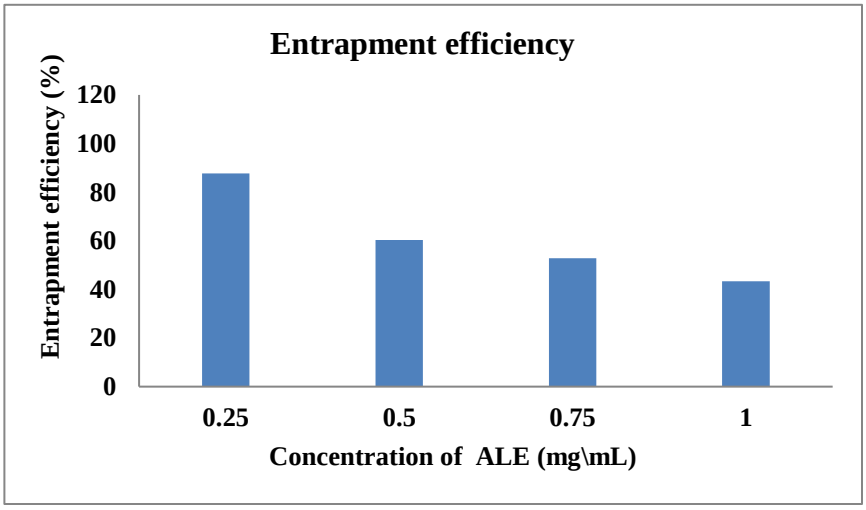

Fig. 1: Entrapment efficiency (%)

In vitro drug release study

The cumulative release of the ALE from CSNPs was studied in dialysis bag containing PBS solution at pH 7.4. The released amount of ALE was calculated by comparing the absorbance of the drug at 265 nm by UV–vis spectroscopy with the earlier measured calibration curves with a dilution series. Finally, the cumulative percent of drug released from CSNPs was plotted against time. *In vitro* drug release studies showed a controlled and sustained release of ALE from CSNPs (91.3%) within five and half hours (Fig.2).

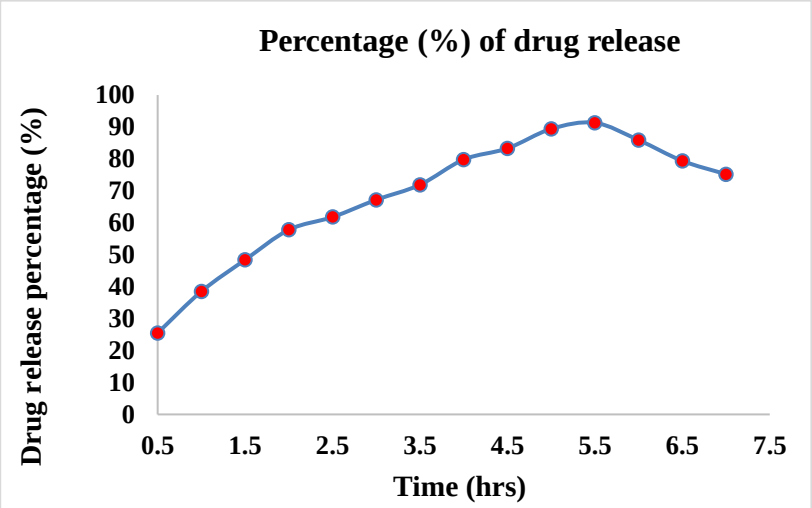

Fig. 2: *In vitro* drug release percentage of ALE from ALE CSNPs

In vitro drug release kinetics

In vitro drug release profile of ALE CSNPs indicates that 50% of the drug was released within 2 hours. After five and half hours, 91.3 % of the drug was released with slow and sustained manner. In order to analyze the *in vitro* release data and to evaluate the drug release kinetics, four mathematical models such as zero order, first order, Higuchi model and Korsmeyer–Peppas have been used **(Fig. 3)**. The values of correlation coefficient of kinetics models are presented in Table 1. The R^2 value obtained from the Higuchi model is found to be greater (0.99) than those of other models. It indicates the release mechanism of ALE from CSNPs has been taking place following dissolution process.

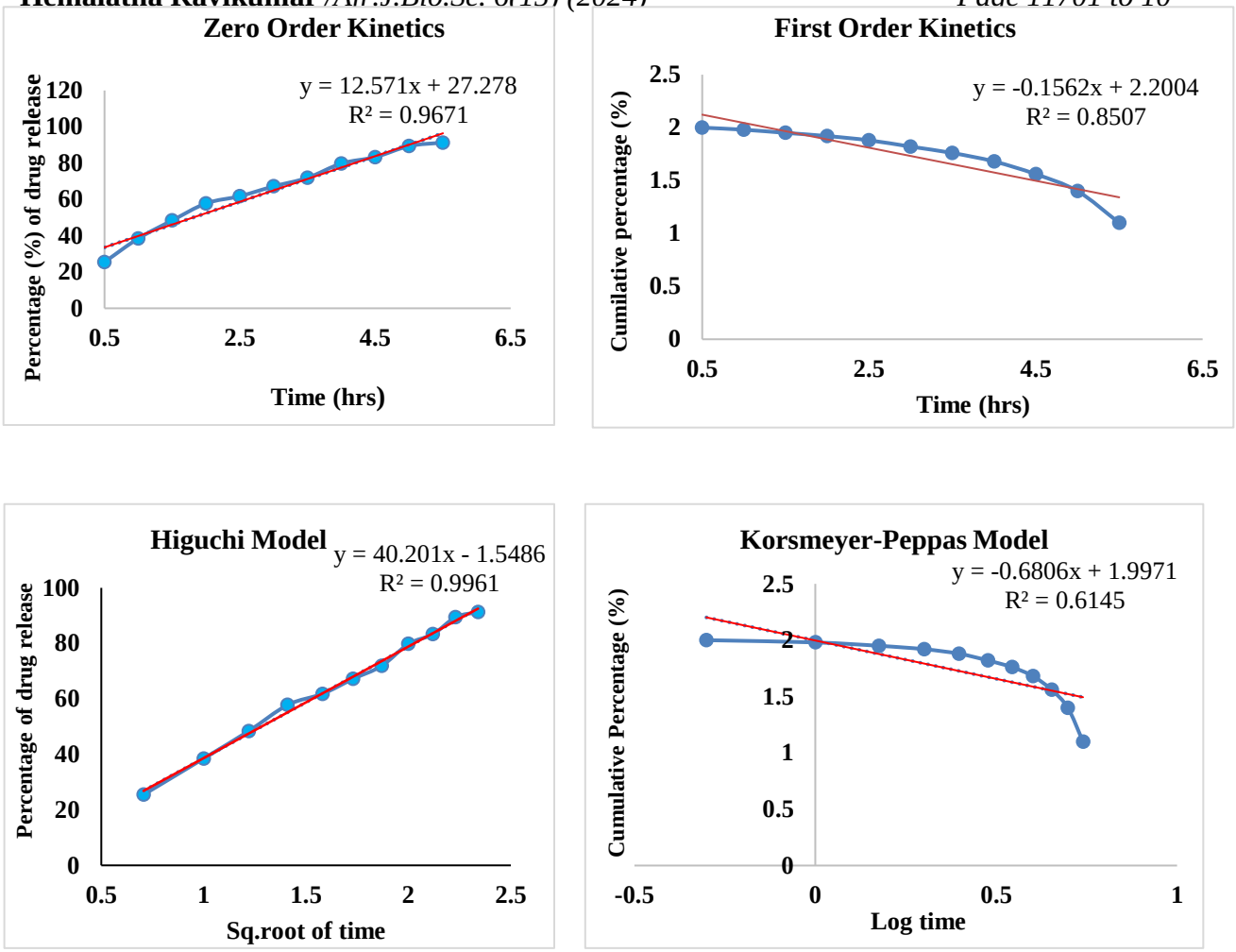

Fig 3: *In vitro* drug release kinetics plots

Table 1: Correlation coefficients and kinetic constants of different kinetics models for ALE CSNPs.

Kinetic Models	Encapsulated ALE CSNPs		
	R^2	Slope	Intercept
Zero order kinetics	0.9671	12.571	27.278
First order kinetics	0.8507	-0.1562	2.2004
Higuchi Model	0.9961	40.201	1.5486
Korsmeyer-Peppas Model	0.6145	-0.6806	1.9971

Ultraviolet Visible (UV – Vis)

To identify the absorbance peaks of both CSNPs and ALE CSNPs, a UV/Vis spectrophotometer scans were taken over the wavelength range of 200 to 800 nm. The strong surface plasmon resonance (SPR) centered at 250 nm was attributed to both CSNPs and ALE CSNPs (Fig.4A).

Fourier Transform Infrared (FTIR) Spectroscopy

FTIR analysis was carried out to identify functional groups present in the ALE CSNPs complex. FTIR spectrum of ALE CSNPs is compared with the FTIR spectrum of CSNPs (Fig. 4B). The spectra obtained for CSNPs and ALE CSNPs showed thirteen and eighteen peaks with various functional groups, respectively. Seven functional groups were found common for both. The FTIR spectrum of CSNPs exhibits characteristic bands assigned to the δ-lactone at the wavelength of 1742.05 cm^{-1}, aldehyde at the wavelength of 1385.85 cm^{-1}, alkyl aryl ether at the wavelength of 1222.65 cm^{-1} and 1,2,4-trisubstituted aromatic compound at the wavelength of

886.131 cm^{-1}. There were six characteristic bands unique to ALE CSNPs such as conjugated acid halide at the wavelength of 1747.19 $cm^{-1,}$ imine/oxime at the wavelength of 1644.98 cm^{-1}, carboxylic acid at the wavelength of 1420.32 cm^{-1}, phenol at the wavelength of 1375.96cm^{-1}, sulfonamide at the wavelength of 1314.25 cm^{-1} and anhydride at the wavelength of 1045.94 cm^{-1}.

X-ray diffraction (XRD)

The XRD pattern of CSNPs showed the highest peaks in 2θ range with various crystal planes i.e 20.96° (223), 21.96° (390), 22.60° (455), 23.04° (399) and 25.10° (683). ALE CSNPs exhibited the presence of several crystal peaks i.e 21.98° (389), 22.26° (403), 24.04° (733), 29.98° (560) and 30.08° (643) situated at angles (2θ). The amorphous nature of the XRD pattern was observed for both samples. The average size of the CSNPs and ALE CSNPs were 22.3 nm and 29.3 nm, respectively, which was determined using the Debye-Scherrer equation (**Fig. 4C).**

Zeta potential, Dynamic light scattering and Polydispersity index

The zetapotential of CSNPs and ALE CSNPs were + 10.67 mV and + 28.40 mV, respectively (**Fig. 4D)**. The mean diameter and poly dispersity index (PDI) of the tested nanoparticles in the water medium were observed by the DLS method and the results are described in **fig.4E**. The average diameter of CSNPs and ALE CSNPs are found to be 240 ± 0.5 nm and 260 ± 1.5 nm, respectively. PDI for CSNPs and ALE CSNPs were 0.22 and 0.35, respectively.

Scanning Electron Microscopy (SEM)

The surface morphology of the CSNPs and ALE CSNPs was determined by SEM analysis. There was a large amount of spherical shaped and well separated nanoparticles found for both the samples **(Fig.4F).** The size of crystalline structure was calculated using Debye–Scherrer equation. The mean size of CSNPs was found smaller (56.88 nm) than the ALE loaded CSNPs (64.53 nm).

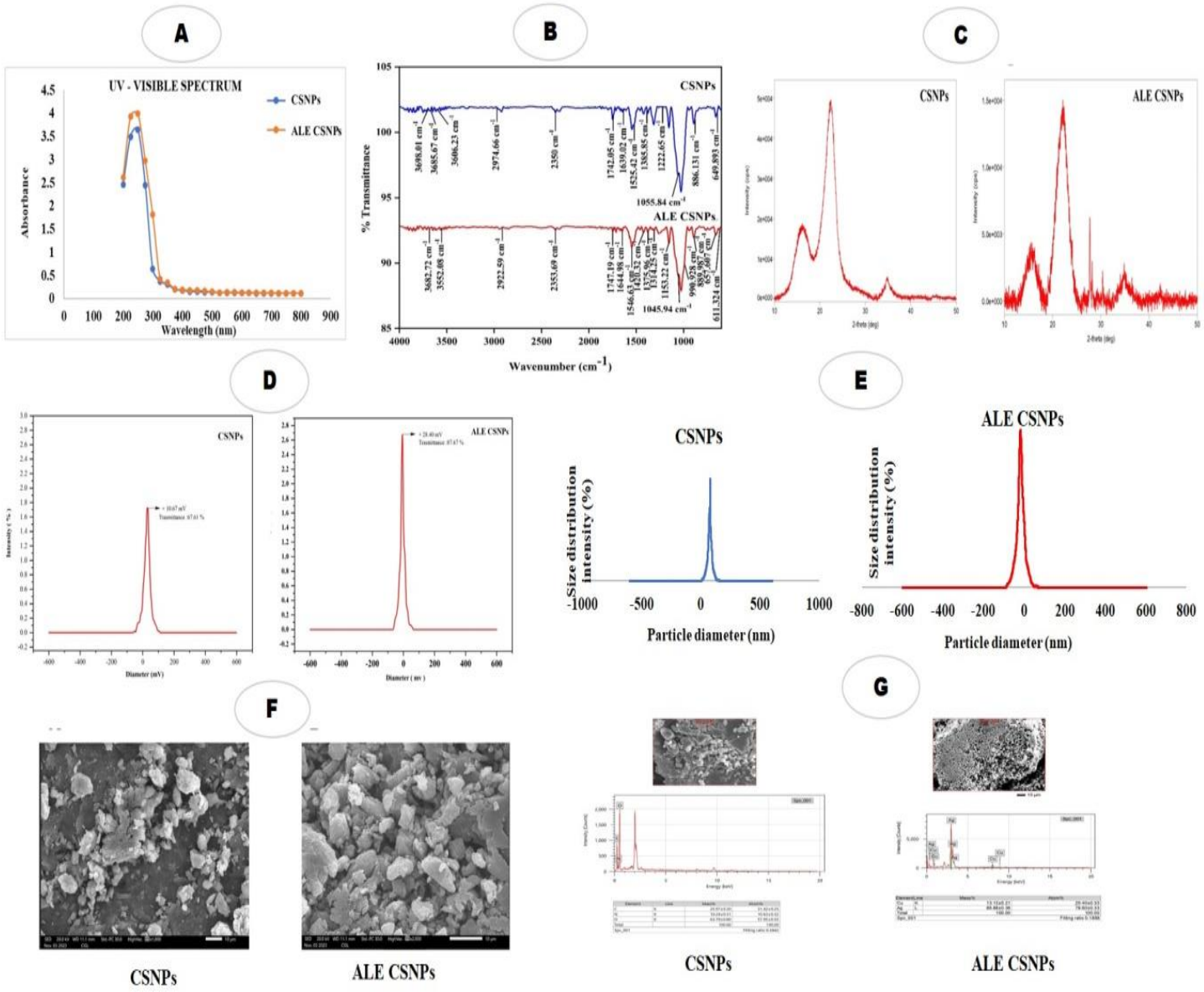

Energy-dispersive X-ray (EDAX)

The EDAX spectra analysis of CSNPs and ALE CSNPs showed the presence of carbon (C), oxygen (O) and nitrogen (N) as main elements **(Fig. 4G)**. The presence of signals for sliver (Ag) and copper (Cu) indicates the impurities of the samples.

Fig. 4: A) UV Visible spectra of CSNPs and ALE CSNPs; B) FTIR spectra CSNPs and ALE CSNPs; C) X-ray diffraction Pattern of CSNPs and ALE CSNPs; D) Zeta potential of CSNPs and ALE CSNPs; E) DLS of CSNPs and ALE CSNPs; F) SEM micrograph of CSNPs and ALE CSNPs and G) EDAX analysis of CSNPs and ALE CSNPs.

Cell inhibition and Cell morphological analysis

In this study, the effect of different concentrations of ALE CSNPs on cancerous cells was assessed by both morphological analysis and MTT assay. After 24 h treatment, of various concentrations of ALE CSNPs, the higher cell inhibitory percentage i.e 92.9% against PC3 cell line was found at 100 µg/mL concentration compared to standard Doxorubicin **(Fig. 5-I**). At this same concentration, notable impact on cancer cell morphology such as the cell membrane disruption and nuclear condensation were observed in cells treated with ALE CSNPs compared to CSNPs, standard Doxorubicin and ALE treated cancer cells (**Fig. 5-II a-b).**

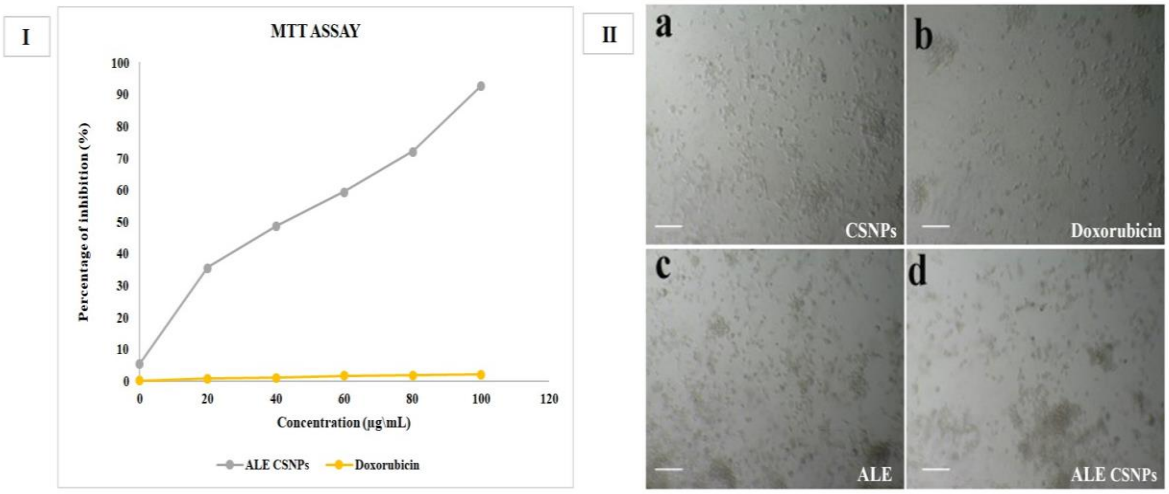

Fig.5: I) Effect of ALE CSNPs and standard Doxorubicin on PC3 cells inhibition percentage. PC3 cells were treated with 20, 40, 60, 80 and 100 µg/mL of ALE CSNPs for 24 hr and their viability were examined by MTT assay. Data are reported as the mean ± SEM (n=3) ; II) a-b Morphological changes of PC3 cell line treated with CSNPs, Doxorubicin, ALE and ALE CSNPs for 24 hrs.

Cell cycle analysis by Flow cytometry

Flow Cytometric analysis revealed that PC3 cells treated with ALE CSNPs exhibited significantly increased percentage of obstructed cells at G0/G1 phase after 24 h, whereas the percentages were significantly decreased at S and G2/M phases. These results indicated that following exposure to ALE CSNPs, cells were impeded in their cycle progression **(Fig. 6 A-D)**.

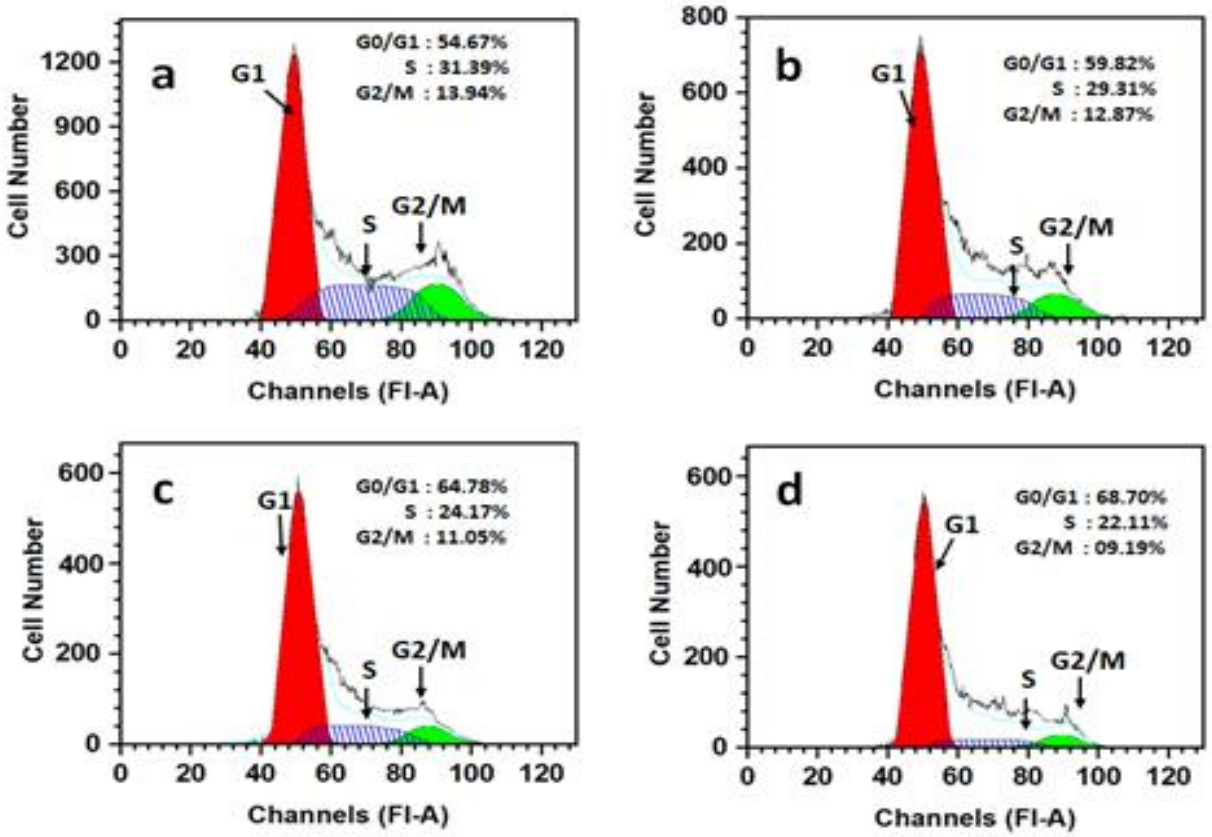

Fig 6: Cell cycle analysis of (A) CSNPs (B) Doxorubicin (C) Plant extract (D) ALE CSNPs. Quantification of the effects of treatment on the cell cycle distribution as determined via flow cytometry.

*** P<0.05 vs. control and Chitosan nanoparticles.**

Discussion

Cancer is one of the major causes of death in various countries and is one of the main problems in the current century [15]. Conventional radiation and chemotherapies are associated with severe side effects in addition to being unduly expensive. Herbal medicines have acquired very high demand since the early civilization because of their effectuality against several diseases comprising cancer. Research conducted by different people suggests the extensive potential of various plant extracts used in traditional as well as folk medicine and phytochemicals thereof with a peculiar mode of action as an effective remedy for detrimental diseases like prostate cancer [16,17] In the current study, we investigated the cytotoxicity and cell cycle arrest of human prostate cancer cells by using chitosan nanoparticles encapsulated *A. serpyllifolia* aqueous extract.

In general, *A. serpyllifolia* claims to treat antibacterial, anti-dote, anticancer, anti-ulcer, anti-inflammatory [18] and anti-diabetic activities [19]. Phenolics and andrographolide of *A. serpyllifolia* are the main bioactive compounds acting on its anticancer property [20]. Chitosan is a linear co-polymer composed of β-(1–4) linked D-glucosamine and N-acetyl-D-glucosamine units and is currently drawing attention as a promising raw material in pharmaceutical, medicinal and agricultural applications [21]. In the present investigation, aqueous extract of *A. serpyllifolia* (ALE) at various concentrations were encapsulated with 2% (w/v) chitosan nanoparticles (ALE CSNPs). The encapsulation or entrapment percentage was ranged from 43.39% to 87.73%. The highest EE% was obtained for 0.25 mg/mL concentration of ALE CSNPs. Increasing the concentration of plant extract caused a decrease of EE% from 0.5 to 1.0 mg/mL. The reason behind is the excess level of plant extract cannot be absorbed by chitosan nanoparticles due to accomplishment of saturation level. Previous studies have also reported similar results [22]. In general, drugs with higher entrapment efficiency are able to enter nanocarrier systems more

easily due to their hydrophobic nature. It is also due to ionic interaction between the CSNPs and TPP [23].

Our investigation on *in vitro* drug release studies reveals that a characteristic biphasic release tendency i.e release of ALE from CSNPS was 57.8 ± % within 2 hours (initial burst) and was 91.3± % within five and half hours (sustained drug release). These results are in parallel with those reported in a recent study [24]. In order to analyze the *in vitro* release data and to evaluate the drug release kinetics, four mathematical models such as zero order, first order, Higuchi model and Korsmeyer–Peppas have been used. The mechanism of drug release from CSNPs involves various mechanisms such as desorption, erosion, degradation, reabsorption and diffusion [25,26]. The drug release kinetics from drug carrier is vital in preclinical development and will serve as the basis for evaluation of drug formulations and regulatory approvals. Prediction of *in vivo* drug release through *in vitro* techniques for nano formulations is becoming widely developed [27]. The diffusion-controlled release kinetics was explored using the zero-order, first-order, and Higuchi models. Mathematical models have many advantages, involving predicting drug release mechanisms, helping in formulation development and fabricating controlled drug release systems [28]. In the present study, the R^2 value obtained from the Higuchi model is found to be greater (0.99) than those of other models. This result suggested that ALE release at pH 7.4 from ALE CSNPs complex follows the Higuchi model kinetics. It also indicates that ALE is released by diffusion process [29].

To identify the absorbance peaks of both CSNPs and ALE CSNPs, a UV/Vis spectrophotometer scans were taken over the wavelength range of 200 to 800 nm. The strong surface plasmon resonance (SPR) centered at 250 nm was ascribed to both CSNPs and ALE CSNPs (Fig. 4A). It was earlier reported that the UV–visible spectrum of chitosan nanoparticles was ranged between 200 and 322 nm due to the presence of the C=O functional group [30].

FTIR analysis shows the characteristic bands for chitosan nanoparticles (δ-lactone, Aldehyde, Alkyl aryl ether and 1,2,4-trisubstituted aromatic compound) and for ALE CSNPs (Conjugated acid halide, Imine/oxime, Carboxylic acid, Phenol, Sulfonamide and Anhydride). The presence of carboxylic acid and phenols in the plant extract are involved in the interaction of phosphoric ammonium ions of chitosan nanoparticles [31]. XRD analysis show some characteristic bands for CSNPs (455, 399, 683) and ALE CSNPs (733, 560, 643) in their diffractograms at different angles. No significant difference was found between diffractograms of both. However, broadened peaks were found in ALE CSNPs compared to CSNPs which confirmed the amorphous nature of CSNPs and successful encapsulation of ALE within CSNPs. A similar observation was made by Piran [32]. who showed the increased antioxidant activity of green tea extract encapsulated in chitosan-citrate nanogel. In the present study, free chitosan nanoparticles showed a particle size of 240±0.5 nm and the size of ALE encapsulated chitosan nanoparticles is of 260± 1.5 nm during DLS test. The size of the particles increases due to interaction of plant extract with chitosan nanoparticles. Zeta potential value indicates the surface charge of the nanoparticles. In the present study, ALE CSNPs has higher positive zeta potential value (+ 28.40 mV) compared to CSNPs (+ 10.67 mV). The higher zeta potential value indicates the stability of the chitosan nanoparticles. Polydispersity index (PDI) value, ranging from 0 to 1 determines the homogeneity of the nanoparticles. In the present investigation, PDI value observed for CSNPs and ALE CSNPs are 0.22 and 0.35 respectively. (Manne *et al*., 2020; Mondéjar-López *et al*., 2022). In this study, the SEM analysis shows the topography of CSNPs and ALE loaded CSNPs. The unloaded separated free chitosan nanoparticles have a smaller size whereas plant extract loaded unglued chitosan nanoparticles have a larger size which may due to encapsulation of plant extract. These results are found similar with the findings of previous researchers [33,34]. Energy-dispersive X-ray spectroscopy (EDAX) analysis was used to

investigate the chemical composition and principal constituents of biosynthesized CSNPs [35In this present study, EDAX results inferred the number of different constituents (carbon, oxygen and nitrogen) present in the nanocomposite.

In the present study, it is clear that PC3 cancer cells treated with various concentrations of ALE CSNPs lose their capacity to proliferate in a dose dependent manner after 24 hrs during MTT assay. The higher cell inhibitory percentage was found at 100 µg/ml concentration with 24 µg/mL IC_{50} value. These findings are in agreement with earlier studies describing genistein and anti-inflammatory drug celecoxib loaded nanoliposome formulation [36], curcumin loaded lipid nanoparticles [37] and sodium butyrate loaded PEG, folic acid and chitosan mediated nano complex [38] are found to be suppressing prostate cancer cell growth via induction of apoptosis and autophagy during cellular phases.

Cell cycle is a series of events that controls the self-replication of cells. One or more cell-cycle checkpoint defects are involved in most of the cancer types including prostate cancer [39] The results of our study showed that the anti-tumor effect of ALE CSNPs significantly hampered the PC3 cell lines in S- phase and led to less accumulation of obstructed cell lines in G2-M phase [40].

CONCLUSION

In conclusion, our results indicate that ALE CSNPs has cytotoxic activity in PC3 cancerous cells. This present study has successfully developed the ALE CSNPs as a promising drug delivery system using chitosan nanocarrier for targeted release of *A. serpyllifolia* leaf aqueous extract to PC3 cell lines. The characterization studies of plant extract encapsulated chitosan nanoparticles confirmed the successful loading of plant drug onto CSNPs. Some biomedical tests like MTT assay and analytical DNA flow cytometry have been applied for analyzing the prostate cancer cell growth destruction. Outputs have noticeably confirmed the potential performance of ALE CSNPs in the inhibition of PC3 cancer cells. The outcome of the investigation provided a ground base to initiate *in vivo* experiments to assess the efficiency of ALE CSNPs on animal models and also to perform some advanced studies to understand the effective molecular mechanisms of ALE CSNPs behind prostate cancer suppression.

Acknowledgement

The authors duly acknowledge funding agencies i.e DST-FIST and DST-PURSE, India for providing all the instrumentation facilities for carrying out the research work in the Dept. of Botany, Bharathiar University, Coimbatore, Tamil Nadu, India.

Conflicts of interest

The authors declare that there is no conflict of interest.

Funding Source

Nil

References

1. Wang, K., Wu, X., Wang, J., & Huang, J. (2013). Cancer stem cell theory: therapeutic implications for nanomedicine. *International Journal of Nanomedicine*, 899-908. https://doi.org/10.2147/ijn.s38641
2. Sahyon, H. A., & Al-Harbi, S. A. (2020). Antimicrobial, anticancer and antioxidant activities of nano-heart of Phoenix dactylifera tree extract loaded chitosan nanoparticles: In vitro and in vivo study. *International journal of biological macromolecules*, *160*, 1230-1241. https://doi.org/10.1016/j.ijbiomac.2020.05.224
3. Lakshmanan, V. K., Snima, K. S., Bumgardner, J. D., Nair, S. V., & Jayakumar, R. (2011). Chitosan-based nanoparticles in cancer therapy. *Chitosan for biomaterials I*, 55-91. https://doi.org/10.1007/12_2011_132
4. Madhankumar, R., & Murugesan, S. (2019). Phytochemical, gas chromatography with mass spectrometry analysis of Andrographis serpyllifolia methanol leaf extract and its antioxidant and antibacterial activities. *Asian J Pharm Clin Res*, *12*(3), 343-347. https://doi.org/10.22159/ajpcr.2019.v12i3.30618
5. Hansiya, V. S., & Geetha, N. (2021). In vitro anti-venom potential of various solvent based leaf extracts of Andrographis serpyllifolia (Rottler ex Vahl) Wight against Naja naja and Daboia russelli. *Journal of ethnopharmacology*, *269*, 113687. https://doi.org/10.1016/j.jep.2020.113687
6. Venkateshaiah, S. U., Jayaram, S., & Dharmesh, S. M. (2009). Antiproliferative, antioxidant and cyto/DNA protective properties in Andrographis serpyllifolia: role of andrographolide and phenolic acids. *Journal of Complementary and Integrative Medicine*, *6*(1). http://dx.doi.org/10.2202/1553-3840.1252
7. Jayaram, S., & Dharmesh, S. M. (2011). Antiproliferative effect of antioxidative free and bound phenolics from Andrographis serpyllifolia. *Free Radicals and Antioxidants*, *1*(3), 56-65. https://doi.org/10.5530/ax.2011.3.8
8. Hamdan, D. I., Tawfeek, N., El-Shiekh, R. A., Khalil, H. M., Mahmoud, M. Y., Bakr, A. F., ... & El-Shazly, A. M. (2022). Salix subserrata bark extract-loaded chitosan nanoparticles attenuate neurotoxicity induced by sodium arsenate in rats in relation with HPLC–PDA-ESI–MS/MS profile. *AAPS PharmSciTech*, *24*(1), 15. https://doi.org/10.1208/s12249-022-02478-4
9. Bagyalakshmi, J., & Haritha, H. (2017). Green synthesis and characterization of silver nanoparticles using Pterocarpus marsupium and assessment of its in vitro Antidiabetic activity. *Am. J. Adv. Drug Deliv*, *5*(3). http://www.imedpub.com/advanced-drug-delivery/
10. Sultan, M., Mohamed, O. A., El-Masry, H. M., & Taha, G. (2023). Fabrication and evaluation of antimicrobial cellulose/Arabic gum hydrogels as potential drug delivery vehicle. *International Journal of Biological Macromolecules*, *242*, 125083. https://doi.org/10.1016/j.ijbiomac.2023.125083
11. Dash, T. K., & Konkimalla, V. B. (2012). Poly-ϵ-caprolactone based formulations for drug delivery and tissue engineering: A review. *Journal of Controlled Release*, *158*(1), 15-33. https://doi.org/10.1016/j.jconrel.2011.09.064
12. Paarakh, M. P., Jose, P. A., Setty, C. M., & Peterchristoper, G. V. (2018). Release kinetics–concepts and applications. *International Journal of Pharmacy Research & Technology (IJPRT)*, *8*(1), 12-20. https://doi.org/10.31838/ijprt/08.01.02

13. Lockwood, W. W., Zejnullahu, K., Bradner, J. E., & Varmus, H. (2012). Sensitivity of human lung adenocarcinoma cell lines to targeted inhibition of BET epigenetic signaling proteins. *Proceedings of the National Academy of Sciences*, *109*(47), 19408-19413. https://doi.org/10.1073/pnas.1216363109
14. Benitez, D. A., Pozo-Guisado, E., Alvarez-Barrientos, A., Fernandez-Salguero, P. M., & Castellón, E. A. (2007). Mechanisms involved in resveratrol-induced apoptosis and cell cycle arrest in prostate cancer—derived cell lines. *Journal of andrology*, *28*(2), 282-293. https://doi.org/10.2164/jandrol.106.000968
15. Torre, L. A., Bray, F., Siegel, R. L., Ferlay, J., Lortet-Tieulent, J., & Jemal, A. (2015). Global cancer statistics, 2012. *CA: a cancer journal for clinicians*, *65*(2), 87-108. https://doi.org/10.3322/caac.21262
16. Cragg, G. M., & Newman, D. J. (2013). Natural products: a continuing source of novel drug leads. *Biochimica et Biophysica Acta (BBA)-General Subjects*, *1830*(6), 3670-3695. https://doi.org/10.1016/j.bbagen.2013.02.008
17. Seca, A. M., & Pinto, D. C. (2018). Plant secondary metabolites as anticancer agents: successes in clinical trials and therapeutic application. *International journal of molecular sciences*, *19*(1), 263. https://doi.org/10.3390%2Fijms19010263
18. Krishnaswamy, S., & Kushalappa, B. A. (2018). Systematic Review and Meta-analysis of Andrographis serpyllifolia (Rottler ex Vahl) Wight: An Ethno-pharmaco-botanical Perspective. *Pharmacognosy Journal*, *10*(6s). http://dx.doi.org/10.5530/pj.2018.6s.3
19. Sanjeevaiah, N., & Jithan, A. (2013). Pharmacological screening of A. serpyllifolia For antidiabetic activity. *Int. J. Adv. Pharma*, *2*, 2277-4688. https://doi.org/10.22159/ajpcr.2019.v12i3.30618
20. Venkateshaiah, S. U., Jayaram, S., & Dharmesh, S. M. (2009). Antiproliferative, antioxidant and cyto/DNA protective properties in Andrographis serpyllifolia: role of andrographolide and phenolic acids. *Journal of Complementary and Integrative Medicine*, *6*(1). http://dx.doi.org/10.2202/1553-3840.1252
21. Hosseinnejad, M., & Jafari, S. M. (2016). Evaluation of different factors affecting antimicrobial properties of chitosan. *International journal of biological macromolecules*, *85*, 467-475. https://doi.org/10.1016/j.ijbiomac.2016.01.022
22. Keawchaoon, L., & Yoksan, R. (2011). Preparation, characterization and in vitro release study of carvacrol-loaded chitosan nanoparticles. *Colloids and surfaces B: Biointerfaces*, *84*(1), 163-171. https://doi.org/10.1016/j.colsurfb.2010.12.031
23. Ahmad, N., Khan, M. R., Palanisamy, S., & Mohandoss, S. (2023). Anticancer drug-loaded chitosan nanoparticles for in vitro release, promoting antibacterial and anticancer activities. *Polymers*, *15*(19), 3925. https://doi.org/10.3390/polym15193925
24. Ahamad, Z., Ahmed, M., Mashkoor, F., & Nasar, A. (2023). Chemically modified Azadirachta indica sawdust for adsorption of methylene blue from aqueous solutions. *Biomass Conversion and Biorefinery*, 1-18. http://dx.doi.org/10.1007/s13399-023-04161-5
25. Jain, A., Agarwal, A., Majumder, S., Lariya, N., Khaya, A., Agrawal, H., ... & Agrawal, G. P. (2010). Mannosylated solid lipid nanoparticles as vectors for site-specific delivery of an anti-cancer drug. *Journal of Controlled Release*, *148*(3), 359-367. https://doi.org/10.1016/j.jconrel.2010.09.003

26. Mariadoss, A. V. A., Vinayagam, R., Senthilkumar, V., Paulpandi, M., Murugan, K., Xu, B., ... & David, E. (2019). Phloretin loaded chitosan nanoparticles augments the pH-dependent mitochondrial-mediated intrinsic apoptosis in human oral cancer cells. *International journal of biological macromolecules*, *130*, 997-1008. https://doi.org/10.1016/j.ijbiomac.2019.03.031
27. D'Addio, S. M., Bukari, A. A., Dawoud, M., Bunjes, H., Rinaldi, C., & Prud'homme, R. K. (2016). Determining drug release rates of hydrophobic compounds from nanocarriers. *Philosophical transactions of the royal society a: mathematical, physical and engineering sciences*, *374*(2072), 20150128. https://doi.org/10.1098/rsta.2015.0128
28. D'Souza, S. (2014). A review of in vitro drug release test methods for nano-sized dosage forms. *Advances in pharmaceutics*, *2014*(1), 304757. https://doi.org/10.1155/2014/304757
29. Tığlı Aydın, R. S., & Pulat, M. (2012). 5-Fluorouracil encapsulated chitosan nanoparticles for pH-stimulated drug delivery: Evaluation of controlled release kinetics. *Journal of Nanomaterials*, *2012*(1), 313961. https://doi.org/10.1155/2012/313961
30. Duraisamy, N., Dhayalan, S., Shaik, M. R., Shaik, A. H., Shaik, J. P., & Shaik, B. (2022). Green synthesis of chitosan nanoparticles using of Martynia annua L. ethanol leaf extract and their antibacterial activity. *Crystals*, *12*(11), 1550. https://doi.org/10.3390/cryst12111550
31. Singh, J., Dutta, T., Kim, K. H., Rawat, M., Samddar, P., & Kumar, P. (2018). 'Green'synthesis of metals and their oxide nanoparticles: applications for environmental remediation. *Journal of nanobiotechnology*, *16*, 1-24. https://doi.org/10.1186/s12951-018-0408-4
32. Piran, N., Teall, T. L., & Counsell, A. (2020). The experience of embodiment scale: Development and psychometric evaluation. *Body image*, *34*, 117-134. https://doi.org/10.1016/j.bodyim.2020.05.007
33. Hosseini, S. F., Zandi, M., Rezaei, M., & Farahmandghavi, F. (2013). Two-step method for encapsulation of oregano essential oil in chitosan nanoparticles: preparation, characterization and in vitro release study. *Carbohydrate polymers*, *95*(1), 50-56. https://doi.org/10.1016/j.carbpol.2013.02.031
34. Manne, A. A., Kumar, A., Mangamuri, U., & Podha, S. (2020). Pterocarpus marsupium Roxb. heartwood extract synthesized chitosan nanoparticles and its biomedical applications. *Journal of Genetic Engineering and Biotechnology*, *18*(1), 19. https://doi.org/10.1186/s43141-020-00033-x
35. Hussein, M. A. M., Grinholc, M., Dena, A. S. A., El-Sherbiny, I. M., & Megahed, M. (2021). Boosting the antibacterial activity of chitosan–gold nanoparticles against antibiotic–resistant bacteria by Punicagranatum L. extract. *Carbohydrate polymers*, *256*, 117498. https://doi.org/10.1016/j.carbpol.2020.117498
36. Tian, J., Guo, F., Chen, Y., Li, Y., Yu, B., & Li, Y. (2019). Nanoliposomal formulation encapsulating celecoxib and genistein inhibiting COX-2 pathway and Glut-1 receptors to prevent prostate cancer cell proliferation. *Cancer Letters*, *448*, 1-10. https://doi.org/10.1016/j.canlet.2019.01.002
37. Tanaudommongkon, I., Tanaudommongkon, A., Prathipati, P., Nguyen, J. T., Keller, E. T., & Dong, X. (2020). Curcumin nanoparticles and their cytotoxicity in docetaxel-

resistant castration-resistant prostate cancer cells. *Biomedicines*, *8*(8), 253. https://doi.org/10.3390%2Fbiomedicines8080253

38. Zamanvaziri, A., Meshkat, M., Alazmani, S., Khaleghi, S., & Hashemi, M. (2023). Targeted PEGylated chitosan nano-complex for delivery of sodium butyrate to prostate cancer: an in vitro study. *Technology in Cancer Research & Treatment*, *22*, 15330338231159223. https://doi.org/10.1177%2F15330338231159223
39. Siddiqui, I. A., Saleem, M., Adhami, V. M., Asim, M., & Mukhtar, H. (2007). Tea beverage in chemoprevention and chemotherapy of prostate cancer 1. *Acta Pharmacologica Sinica*, *28*(9), 1392-1408. 10.1111/j.1745-7254.2007.00693.x
40. Jadhav, V., Ray, P., Sachdeva, G., & Bhatt, P. (2016). Biocompatible arsenic trioxide nanoparticles induce cell cycle arrest by p21WAF1/CIP1 expression via epigenetic remodeling in LNCaP and PC3 cell lines. *Life sciences*, *148*, 41-52. https://doi.org/10.1016/j.lfs.2016.02.042